

# In-Band OSNR Monitoring Using Spectral Analysis After Frequency Down-Conversion

Lamia Baker-Meflah, *Student Member, IEEE*, Seb Savory, Benn Thomsen, John Mitchell, *Member, IEEE*, and Polina Bayvel, *Senior Member, IEEE*

**Abstract**—A novel method for simultaneous optical signal-to-noise ratio and chromatic dispersion monitoring in wavelength-division multiplexed 40-Gb/s systems is proposed and demonstrated. This technique has a fast response time of <10 ms, applicable to dynamically reconfigurable networks, and is able to simultaneously monitor multiple impairments across multiple channels.

**Index Terms**—Chromatic dispersion (CD), optical signal-to-noise ratio (OSNR), single sideband (SSB).

## I. INTRODUCTION

**F**UTURE optical networks will evolve from static to dynamically reconfigurable architectures, to meet the increasing bandwidth and service requirements. These networks will require performance monitoring techniques with the following criteria: 1) ideally a single monitor should allow for the measurement of various impairments such as channel power, optical signal-to-noise ratio (OSNR), chromatic dispersion (CD), and polarization-mode dispersion; 2) the response time of the monitor must be compatible with the network switching time allowing for a monitoring on a per-burst basis; 3) multichannel operation is possible, to provide a cost-effective solution.

Advanced optical performance-monitoring techniques such as RF spectrum analysis using clock detection [1], [2] and pilot tones [3] require high-speed detection per channel, and are not cost-effective for multichannel operation. Eye diagram sampling techniques [4] require long processing time (subsecond) preventing monitoring on a per-burst basis; in addition, these methods have a single-channel operation.

In this letter, a novel method for simultaneously monitoring power, OSNR, and CD in 40-Gb/s multichannel systems is proposed and demonstrated. Previously we have demonstrated this technique for CD monitoring [5]. Here, we show that the same setup can also be used to perform per-channel OSNR measurements. The dynamic range and the required acquisition time are assessed. The 10-ms acquisition time of this technique is applicable to dynamically reconfigurable networks. In addition, the use of an electrooptic down-conversion technique that simultaneously down-converts multiple wavelength-division-multiplexing (WDM) channels makes it cost-effective for multichannel operation.

Manuscript received July 18, 2006; revised November 10, 2006. This work was supported in part by EU IST Integrated Project NOBEL (FP6) and EPSRC. The authors are with the Electronic and Electrical Engineering Department, University College London, London WC1E 7JE, U.K. (e-mail: l.baker@ee.ucl.ac.uk).

Color versions of one or more of the figures in this letter are available online at <http://ieeexplore.ieee.org>.

Digital Object Identifier 10.1109/LPT.2006.888971

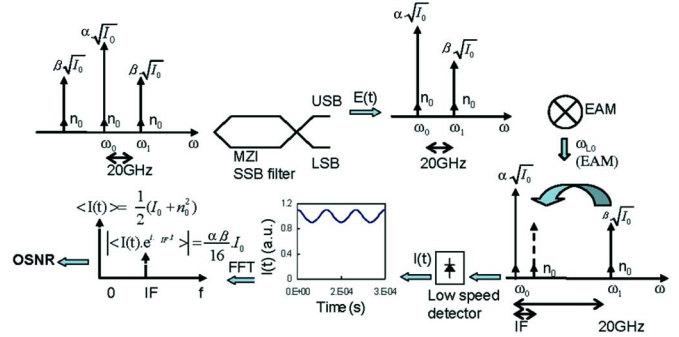


Fig. 1. Principle of the spectral-analysis-based OSNR measurement technique.

## II. CONCEPT AND MATHEMATICAL ANALYSIS

The OSNR measurement principle is schematically shown in Fig. 1. The signal and noise are optically filtered to select the optical carrier and a single sideband (SSB). The SSB signal is then electrooptically heterodyned down to an intermediate frequency (IF) of  $\approx 10$  kHz which is then detected using a low bandwidth (<500 MHz) square-law photodetector. The electrical signal is then digitized and the IF tone is extracted in software with a fast Fourier transform (FFT). Below it is shown that the ratio of the total average power to the amplitude of the IF tone is proportional to OSNR (7).

After the optical down conversion and low-speed detection, the received signal  $I(t)$  is given by

$$I(t) = |E(t)|^2 \cdot G(t) \quad (1)$$

where  $E(t)$  is the filtered signal and noise and  $G(t)$  is the optical modulator transfer function

$$G(t) = \frac{1}{2}(1 + \cos(\omega_{LO} \cdot t))$$

and

$$\omega_{LO} = (\omega_1 - \omega_0) + \omega_{IF}$$

where  $\omega_0$  and  $\omega_1$  are, respectively, the optical frequencies of the carrier and the SSB tone. To illustrate the concept, the filtered SSB optical field can be modelled as two monochromatic tones. The noise associated with this signal is also modelled as two monochromatic tones of equal amplitudes ( $n_o$ ) and random phases ( $\varphi_{n0}, \varphi_{n1}$ ) [6]

$$\begin{aligned} E(t) = & \alpha \cdot \sqrt{I_0} \cdot \cos(\omega_0 \cdot t + \varphi_0) \\ & + \beta \cdot \sqrt{I_0} \cdot \cos(\omega_1 \cdot t + \varphi_1) \\ & + n_0 \cdot \cos(\omega_0 \cdot t + \varphi_{n0}) \\ & + n_0 \cdot \cos(\omega_1 \cdot t + \varphi_{n1}) \end{aligned} \quad (2)$$

where  $I_0 = \langle E^2(t) \rangle_{n_0=0}$  is the total signal power and  $\alpha$  and  $\beta$  determine the amplitude splitting between each tone normalized such that  $(1/2) \cdot (\alpha^2 + \beta^2) = 1 \cdot \alpha \cdot \sqrt{I_0}$  and  $\beta \cdot \sqrt{I_0}$  are the amplitudes of each tone, which depend on the data signal power spectrum and the SSB filter transfer function. The DC and 10-kHz terms of the detected signal  $I(t)$  are

$$\begin{aligned} I(t) = & \frac{I_0}{2} + \frac{n_0^2}{2} + \frac{\alpha \cdot \sqrt{I_0} \cdot n_0}{2} \cdot \cos(\varphi_0 - \varphi_{n0}) \\ & + \frac{\beta \cdot \sqrt{I_0} \cdot n_0}{2} \cdot \cos(\varphi_1 - \varphi_{n1}) \\ & + \frac{\alpha \cdot \beta \cdot I_0}{8} \cdot \cos(\omega_{IF} \cdot t + \varphi_{SSB}) \\ & + \frac{n_0^2}{8} \cdot \cos(\omega_{IF} \cdot t + (\varphi_{n0} - \varphi_{n1})) \\ & + \frac{\alpha \cdot \sqrt{I_0} \cdot n_0}{8} \cdot \cos(\omega_{IF} \cdot t + (\varphi_0 - \varphi_{n1})) \\ & + \frac{\beta \cdot \sqrt{I_0} \cdot n_0}{2} \cdot \cos(\omega_{IF} \cdot t + (\varphi_{n0} - \varphi_1)) \end{aligned} \quad (3)$$

where  $\varphi_{SSB} = \varphi_0 - \varphi_1$ .

The time-averaged detected signal is linearly proportional to the noise power

$$\langle I(t) \rangle = \frac{1}{2} (I_0 + n_0^2) \quad (4)$$

given that terms containing  $\langle \cos(\omega \cdot t) \rangle = 0$  and  $\langle \cos(\varphi_n) \rangle = \langle \sin(\varphi_n) \rangle = 0$  when  $\varphi_n$  is random, time-average to zero.

The components of  $I(t)$  at the IF are extracted using an FFT and after time-averaging this component depends only on the average signal power, and is independent of the noise power. It is also noted that the modulus of the IF tone solely depends on the average signal power and not the relative phase of the carrier and sideband  $\varphi_{SSB}$ , and thus is independent of CD

$$I_T(\omega_{IF}) = \langle I(t) \cdot e^{i\omega_{IF} \cdot t} \rangle = \frac{\alpha \cdot \beta}{16} \cdot I_0 \cdot e^{-i \cdot \varphi_{SSB}}. \quad (5)$$

The ratio ( $R$ ) of the total power (signal and noise) (4) to the IF tone amplitude (signal only) (5) is defined as

$$R = \frac{|I(t)|}{|I(t) \cdot e^{i\omega_{IF} \cdot t}|} = \frac{8}{\alpha \cdot \beta} \cdot \left(1 + \frac{n_0^2}{I_0}\right). \quad (6)$$

This ratio is related to the OSNR as follows:

$$\begin{aligned} \text{OSNR} = & -10 \cdot \text{Log}_{10}(\gamma \cdot \frac{n_0^2}{I_0}) \\ = & -10 \cdot \text{Log}_{10}(\gamma \cdot (\frac{\alpha \cdot \beta}{8} \cdot R - 1)) \end{aligned} \quad (7)$$

where  $\gamma$  is a constant of proportionality, dependent on the effective measurement bandwidth. The OSNR can then be determined from the measurement of  $R$  obtained from the ratio of the total power to the IF tone amplitude. It is noted that one sideband measurement is sufficient for the OSNR monitoring. This technique is suitable for intensity modulated formats with a carrier (i.e., nonreturn-to-zero (NRZ), return-to-zero), and can be adapted to different bit rates by changing the LO frequency.

### III. EXPERIMENTAL SETUP

The experimental setup for the simultaneous OSNR and CD measurement is shown in Fig. 2. In this work, only the OSNR measurement technique is presented. The data signal

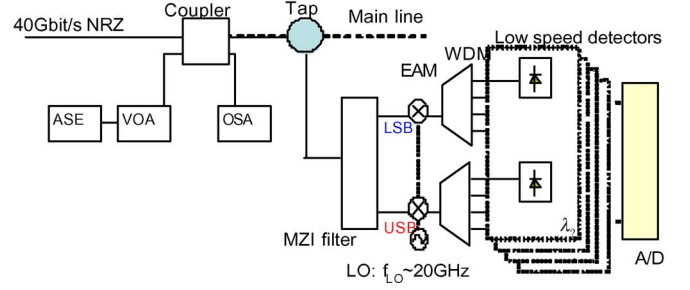


Fig. 2. The 40-Gb/s multichannel OSNR and dispersion monitoring system based on electrooptical mixing.

is a 40-Gb/s  $2^{15} - 1$  pseudorandom binary sequence NRZ. The OSNR is varied with a variable noise loading stage using an amplified spontaneous emission (ASE) source. The main signal is tapped and sent through an optical filter to select the SSB signals. In a WDM system, a Mach-Zehnder interferometer (MZI) filter with a free-spectral range (FSR) equal to a submultiple of the channel spacing can be used (as, e.g., an MZI filter with 50-GHz FSR could be used for a 100- or 200-GHz channel spacing). In this single-channel experiment, the MZI filter used has an FSR of 80 GHz, and a full-width at half-maximum (FWHM) of 0.4 nm. This filter has two outputs and is tuned such that it simultaneously suppresses the lower/upper sideband (LSB/USB) of all the WDM channels on the upper/lower output. The multiwavelength LSB and USB signals are down-converted using two electroabsorption modulators (EAMs) with a 25-GHz bandwidth, and 8-dB insertion loss (IL), where the 20-GHz tone of both sidebands is monitored. The MZI filter transmits one sideband and suppresses the other sideband, forcing the tone frequency (20 GHz) to be equal to a quarter of the MZI filter FSR (80 GHz). The EAMs are driven with a free running local oscillator (LO) using a sinusoidal signal at a frequency  $\omega_{LO}$ , shifted from the sideband offset frequency ( $\omega_1$ ) by  $\sim 10$  kHz ( $\omega_{IF}$ ). The individual channels are then separated by two wavelength-demultiplexer filters and the down-converted LSB and USB signals are detected using two low-speed square law photodetectors with  $1.4\text{-}\mu\text{W/V}$  sensitivity. The signals are then digitized for further processing using an analog-to-digital card (ADC) with a sampling rate of 500 kS/s and 16-bit resolution. This resolution is a limiting factor in measuring low OSNR levels (above 30 dB) with  $-30\text{-dBm}$  input power. The IF is selected to be within the bandwidth of the ADC and lower than unwanted noise tones observed from 20 to 250 kHz.

An FFT is applied to both SSB signals, providing their spectrum which contains the phase and amplitude information at each frequency. A strong tone at the IF frequency of 10 kHz is observed on the FFT spectrum and extracted. The phase measurement of this tone is proportional to CD, whereas its amplitude in conjunction with the total average power provides a measure of OSNR. It is noted that drifts of the local oscillator relative to the signal carrier will vary the IF, but will not have an impact on the monitoring technique since the IF tone is tracked. However, drifts in the IF will limit the integration time. In this experiment, the IF was observed to drift by only 0.1 Hz/s observed over a period of 4 h. In these experiments, the maximum integration time used was 100 ms and so will not be significantly affected by the IF drift.

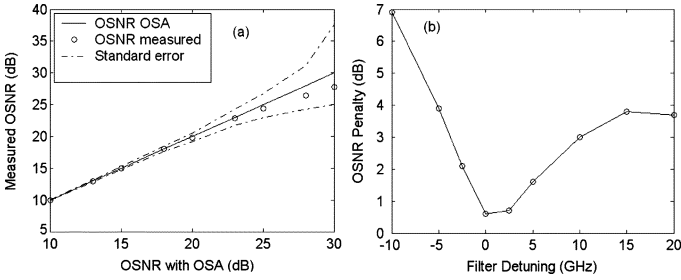


Fig. 3. (a) OSNR monitoring range and accuracy. OSNR measured using an OSA and using the proposed technique (circles). (Input power =  $-30$  dBm; acquisition time = 100 ms.) (b) Impact of the SSB filter detuning on the OSNR measurement accuracy. (OSNR = 20 dB; input power =  $-30$  dBm; acquisition time = 100 ms.)

#### IV. EXPERIMENTAL RESULTS

##### A. Range and Accuracy

The setup described has been analyzed for a single-channel NRZ 40-Gb/s system. In order to minimize component loss, the WDM filter (IL = 5 dB) was replaced by a single-channel filter of 3-dB IL and 1.35-nm FWHM. The OSNR was varied by keeping the signal at a constant power level and attenuating the ASE source as shown in Fig. 2. The effect of varying the OSNR for a constant data signal power, on the amplitude of the extracted IF tone was investigated, was that the tone amplitude is constant and independent of the incoming noise, as predicted by (5).

Fig. 3(a) shows the comparison between the OSNR measured using this technique and the OSNR measured over a 0.5-nm bandwidth (for 40-Gb/s signals) using an optical spectrum analyzer (OSA). The constants  $\alpha$ ,  $\beta$ , and  $\gamma$  [see (7)] have been experimentally obtained in calibrating the system by fitting (7) to the measured  $R$  as a function of the independently measured OSNR using an OSA. The values of these constants are respectively equal to 1.414, 0.01, and 0.1. The maximum error between the measured and the actual OSNR is 0.6 dB over a measurement range of 10–25 dB. The standard error arising from the calibration and experimental uncertainty is also shown in Fig. 3(a). For OSNR values less than 20 dB, the standard error is less than 1 dB; however, the standard error increases considerably for OSNR values higher than 20 dB. The increase in error at large OSNR arises from the error in the measurement of the signal and noise term when the noise is considerably smaller than the signal power. The measurement range could be further improved by reducing the noise in the detection and processing electronics. Fig. 3(b) shows the effect of varying the SSB filter detuning from  $-10$  to 20 GHz on the OSNR measurement penalty. An optimum measurement is obtained with zero detuning corresponding to the SSB filter centered on the 20-GHz tone.

##### B. Sensitivity and Acquisition Time

In order to determine the sensitivity of the system, and thus the required tapped power, the optical input power to the photodetectors was varied from  $-25$  to  $-40$  dBm while the OSNR was kept constant at 20 dB. Fig. 4(a) shows that the RMS error in the measured OSNR increases as the input power decreases.

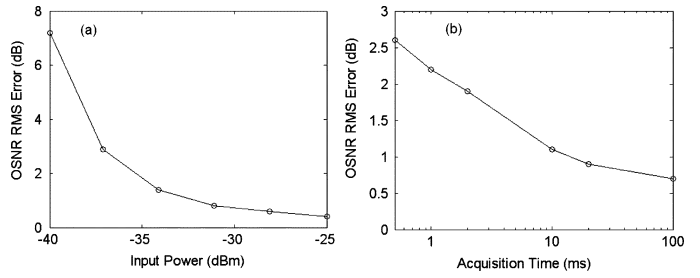


Fig. 4. (a) Impact of the input power level on the OSNR measurement accuracy. (OSNR = 20 dB; acquisition time = 100 ms.) (b) Impact of the acquisition time on the OSNR measurement accuracy. (OSNR = 20 dB; input power =  $-30$  dBm).

From this result, an error of less than 1 dB can be achieved with input powers as low as  $-30$  dBm.

The acquisition time depends on the averaging time required to achieve an acceptable error in the OSNR measurement. Fig. 4(b) shows the effect of reducing the acquisition time from 100 to 1 ms on the RMS error in the OSNR measurement. A 1-dB accuracy was achieved for acquisition times of 10 ms and above. In addition, a preliminary WDM experiment shows that a 20-dB crosstalk does not add any measurable error to the OSNR measurements. This is due to the fact that crosstalk introduces noncoherent light to the channel being measured, which does not impact the measurement of the IF tone.

#### V. SUMMARY

Simultaneous multichannel monitoring of OSNR and CD has been proposed. The performance of this technique was assessed for OSNR measurement in a single-channel 40-Gb/s NRZ system (multiple channel operation will be shown in a later work). The dynamic range of the OSNR measurement was 20 dB. An accuracy of better than 1 dB could be achieved for OSNR values less than 20 dB, optical input powers of  $-30$  dBm, and acquisition times as short as 10 ms. This technique uses two electrooptical modulators to dramatically reduce the number of high-speed components that are required in a multichannel monitoring system. It is suitable for applications in dynamically reconfigurable networks where the monitoring and reconfiguration timescales must be compatible.

#### REFERENCES

- [1] Z. Pan, Q. Yu, Y. Xie, S. A. Havstad, A. E. Willner, D. S. Starodubov, and J. Feinberg, "Chromatic dispersion monitoring and automated compensation for NRZ and RZ data using clock regeneration and fading without adding signaling," in *Proc. OFC*, 2000, vol. 3, pp. WH5/1–WH5/3.
- [2] S. M. Reza, M. Nezam, T. Luo, J. E. McGeehan, and A. E. Willner, "Enhancing the monitoring range and sensitivity in CSRZ chromatic dispersion monitors using a dispersion-biased RF clock tone," *IEEE Photon. Technol. Lett.*, vol. 16, no. 5, pp. 1391–1393, May 2004.
- [3] K. J. Park, "Performance comparisons of chromatic dispersion-monitoring techniques using pilot tones," *IEEE Photon. Technol. Lett.*, vol. 15, no. 6, pp. 873–875, Jun. 2003.
- [4] P. S. Andre, "Asynchronous sampled amplitude histogram model for optical performance monitoring in high speed networks," in *Proc. LEOS*, 2003, pp. 911–912.
- [5] L. Meflah, B. Thomsen, J. Mitchell, and P. Bayvel, "Fast residual chromatic dispersion monitoring for dynamic burst networks," in *Proc. OFC*, 2006, pp. 1–3.
- [6] E. Desurvire, *Erbium-Doped Fiber Amplifiers*. New York: Wiley, 1994, ch. 3.